

# Effects of $\text{Na}^+$ , $\text{K}^+$ , and $\text{Ca}^{2+}$ on the Structures of Anionic Lipid Bilayers and Biological Implication

Huaiyu Yang, Yechun Xu, Zhaobing Gao, Yanyan Mao, Yun Du, and Hualiang Jiang\*

Drug Discovery and Design Center, State Key Laboratory of Drug Research, Shanghai Institute of Materia Medica, Chinese Academy of Sciences, 555 Zuchongzhi Road, Shanghai 201203, China

Received: September 25, 2010; Revised Manuscript Received: October 20, 2010

Ion–membrane interactions are essential to the regulation of cell functions. While numerous molecular dynamics (MD) simulations have been carried out to study the effects of ions on neutral lipid bilayers, few have been conducted on anionic lipid bilayers. Moreover, there is a lack of long-time simulations. Here, submicrosecond MD simulations were performed to investigate the effects of pure cations ( $\text{K}^+$ ,  $\text{Na}^+$ , and  $\text{Ca}^{2+}$ , respectively) on the anionic palmitoyloleylphosphatidylglycerol (POPG) bilayer first. The results reveal how  $\text{K}^+$ ,  $\text{Na}^+$ , and  $\text{Ca}^{2+}$  ions influence the structure of anionic lipid bilayers. In general, cations tighten the anionic lipid bilayer and increase the ordering of the lipids. Subsequently, two MD simulations were carried out to elucidate the effects of extra cations added to the bilayers in addition to counterions. It is found that the extra  $\text{Ca}^{2+}$  ions result in stronger effects on the structures of the lipid bilayer, whereas extra  $\text{Na}^+$  ions do not. Finally, simulations of ion mixture effects on the structure of the POPG bilayer were conducted, and it is observed that  $\text{Ca}^{2+}$ , over  $\text{K}^+$  and  $\text{Na}^+$ , plays a dominant role in affecting the bilayer structures. These results may cast new insights on the distinct functions of  $\text{Ca}^{2+}$  in the biological systems. In addition, our simulations indicate that long-time simulations are necessary to address the effects of ions on lipid bilayer structures.

## Introduction

The cell membranes are selectively permeable and control the movement of substances in and out of cells. The framework of the cell membrane is a lipid bilayer mainly consisting of various kinds of phospholipids that have a hydrophilic headgroup and two hydrophobic tails. Phospholipids are divided into neutral and charged types on the basis of the net charge of the headgroup. Phosphatidylcholine (PC) and phosphatidylethanolamine (PE) are typical neutral lipids, while phosphatidylglycerol (PG), phosphatidylserine (PS), phosphatidylinositol (PI), and cardiolipin are examples of anionic ones.<sup>1,2</sup> Since a wide variety of biological molecules, primarily proteins, are embedded in the lipid bilayer, the components of the lipid bilayer not only determine the structure of the cell membrane but also are involved in a variety of cellular processes such as cell adhesion, ion channel conductance, and cell signaling mediated by membrane proteins.<sup>3–5</sup> The content of charged lipids is a key factor of the components of the lipid bilayer. Charged lipids have strong interactions with surrounding molecules and ions, which further mediate the structures, stabilities, and functions of the cell membranes.<sup>6</sup> Moreover, charged lipids could regulate the activities of many proteins directly by selective interactions with the proteins or indirectly by altering the structural properties of the bilayer.<sup>7–9</sup>

Membrane properties such as aggregation and fusion, surface charges and potentials, structure and mechanical strength, and membrane mobilities as well are tightly associated with ions that are prevalent in both cytosol and the exterior of the membrane with different concentrations.<sup>10–15</sup> Therefore, investigating the interactions of ions, such as  $\text{Na}^+$ ,  $\text{K}^+$ , and  $\text{Ca}^{2+}$ , with the lipid bilayer are considerably interesting and significant.

Molecular dynamics (MD) simulation provide a powerful tool for investigating the interactions between ions and lipid bilayers at the atomic level. Numerous MD simulations have been carried out to study the effects of ions on the structures and dynamics of the neutral lipid bilayers.<sup>16–24</sup> It has been observed that ions do have an impact on the structural properties of lipid bilayer. Some predictions based on the MD simulation results have been experimentally verified.<sup>16,25–28</sup> However, rare MD simulations have been conducted on the anionic lipid bilayers.<sup>29–35</sup> Moreover, except  $\text{Na}^+$ , the effects of other cations, such as  $\text{K}^+$  and  $\text{Ca}^{2+}$  ions, as well as the mixture of different cations on the structures and dynamics of anionic lipid bilayers have not been well studied yet. In addition, the time scale for the previous MD simulations of the lipid bilayers is generally too short to get more insights of the structure–function relationship of cell membranes.

Here, we report the structures and dynamics of the anionic palmitoyloleylphosphatidylglycerol (POPG) bilayers perturbed by various cations ( $\text{Na}^+$ ,  $\text{K}^+$ , and  $\text{Ca}^{2+}$ ) and their mixtures using submicrosecond MD simulations.  $\text{Na}^+$ ,  $\text{K}^+$ , and  $\text{Ca}^{2+}$  ions are selected since they are the most abundant cations in the physiological environment. First, the effects of a single type of cation,  $\text{Na}^+$ ,  $\text{K}^+$ , or  $\text{Ca}^{2+}$ , as counterions on the lipid bilayer are assessed. Second, excess  $\text{NaCl}$  and  $\text{CaCl}_2$  molecules were added to the simulation systems that originally include enough counterions of  $\text{Na}^+$  and  $\text{Ca}^{2+}$ , respectively. The goal of such simulations are to test whether the effects of  $\text{Ca}^{2+}$  on the lipid bilayer are still similar to those of  $\text{Na}^+$  when more cations are added beside of the existed counterions. Finally, two simulations were run on the systems with the mixture of  $\text{Na}^+$ ,  $\text{K}^+$ ,  $\text{Ca}^{2+}$ , and  $\text{Cl}^-$  ions. To our knowledge, this study, for the first time, investigates the effects of the mixture of cations on structural properties of the lipid bilayers.

\* To whom correspondence should be addressed. Tel: +86-21-50805873. Fax: +86-21-50807088. E-mail: hljiang@mail.shcnc.ac.cn.

**TABLE 1: Number of Ions and Water Molecules, Simulation Time, and Area per Lipid for Seven Simulation Systems**

system	Na <sup>+</sup>	K <sup>+</sup>	Ca <sup>2+</sup>	Cl <sup>-</sup>	water	time (μs)	area (Å <sup>2</sup> )
PG <sub>Na</sub>	128				7176	0.6	51.0
PG <sub>K</sub>		128			7176	0.6	68.2
PG <sub>Ca</sub>			64		7240	0.6	50.6
PG <sub>NaCl</sub>	154			26	7124	0.6	51.4
PG <sub>CaCl<sub>2</sub></sub>			77	26	7201	0.6	49.4
PG <sub>NaKCa</sub>	80	80	40	112	17064	0.7	50.4
PG <sub>NaCa</sub>	80		80	112	17064	0.4	49.3

## Materials and Methods

**Simulation Systems.** Starting from a POPC bilayer containing 128 lipid molecules which was constructed by using the program VMD,<sup>36</sup> the model of POPG bilayer was built by changing the headgroup of PC into PG. Each POPG lipid has one unit of negative charge. Seven simulation systems were designed on the basis of the bilayer composed of 128 POPG lipids and solvated with SPC water molecules.<sup>37</sup> Details of these MD simulation systems are listed in Table 1. Systems PG<sub>Na</sub>, PG<sub>K</sub>, and PG<sub>Ca</sub> were constructed to study the effects of single Na<sup>+</sup>, K<sup>+</sup>, or Ca<sup>2+</sup> ions as counterions. Because the POPG bilayer carries 128 negative charges, 128 Na<sup>+</sup>, 128 K<sup>+</sup>, and 64 Ca<sup>2+</sup> ions were added respectively in systems PG<sub>Na</sub>, PG<sub>K</sub>, and PG<sub>Ca</sub> to ensure electroneutrality of the whole system. To investigate whether extra Na<sup>+</sup> and Ca<sup>2+</sup> ions could result in stronger effects, systems PG<sub>NaCl</sub> and PG<sub>CaCl<sub>2</sub></sub> were built by adding 26 NaCl and 13 CaCl<sub>2</sub> molecules into PG<sub>Na</sub> and PG<sub>Ca</sub>, respectively, in addition to the counterions. Systems PG<sub>NaKCa</sub> and PG<sub>NaCa</sub> were designed to study the effects of mixed cations. PG<sub>NaKCa</sub> contains 80 Na<sup>+</sup>, 80 K<sup>+</sup>, 40 Ca<sup>2+</sup>, and 112 Cl<sup>-</sup> ions. System PG<sub>NaCa</sub> was built on the basis of the snapshot structure of PG<sub>NaKCa</sub> extracted at 0.6 μs from the MD trajectory by replacing 80 K<sup>+</sup> ions with 40 Ca<sup>2+</sup> ions, thereby PG<sub>NaCa</sub> includes 80 Na<sup>+</sup>, 80 Ca<sup>2+</sup>, and 112 Cl<sup>-</sup> ions.

**MD Simulations.** Submicrosecond MD simulations were carried out with GROMACS 4.0,<sup>38</sup> under the NPT and periodic boundary conditions. The last 200 ns MD trajectory for PG<sub>NaCa</sub> and the last 300 ns MD trajectories for other six systems were used for analysis. The simulation protocol and parameters were similar to the previous simulations.<sup>39</sup> The Berger force field<sup>40–43</sup> was applied to the lipids, and the OPLS-AA force field<sup>44</sup> was assigned to water molecules and ions. Two force fields were coupled by applying the half-ε double-pairlist method.<sup>39</sup> The SETTLE algorithm<sup>45</sup> was used to constrain the bond of water molecules, and LINCS<sup>46</sup> was used to constrain all other bond lengths. The time step is 2 fs, and electrostatic interactions were calculated with the Particle Mesh Ewald (PME) algorithm.<sup>47</sup> Cutoffs of 12 Å were used for both PME and van der Walls interactions. The pressure was kept constant by isotropically coupling the system to a pressure bath of 1 bar using the Berendsen<sup>48</sup> method, with a coupling constant of 1.0 ps and a compressibility of  $4.5 \times 10^{-5}$  bar<sup>-1</sup>. Systems were coupled to temperature baths at 310 K using the v-rescale<sup>49</sup> method with a coupling time of 0.1 ps.

## Results

**Structure of POPG.** The chemical structure and the atomic numbering of POPG are displayed in Figure 1A. The structure of the POPG bilayer with Na<sup>+</sup> counterions has been previously simulated by using the software GROMACS with a mixed force field of Berger and GROMOS for the lipids.<sup>33,34,50</sup> It has been noted that in these simulations atoms H6 and O8 of POPG

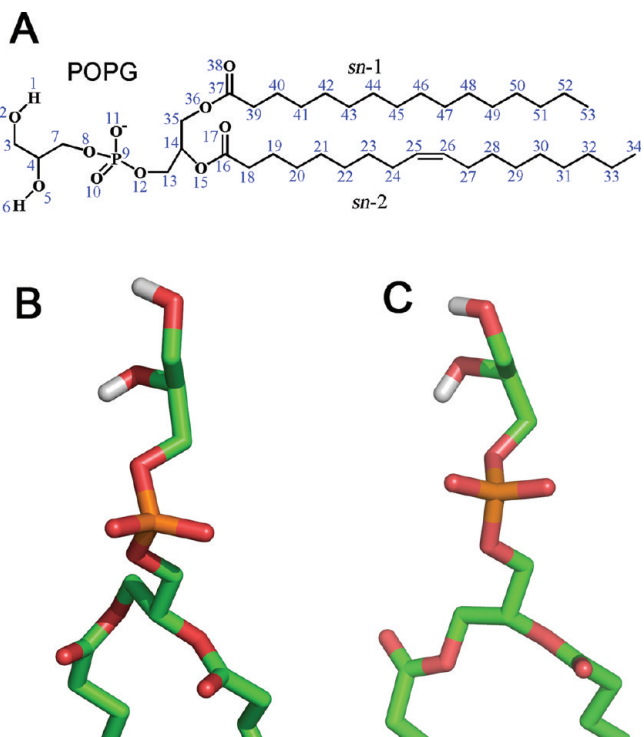


**Figure 1.** (A) Chemical structure and atomic numbering of POPG. (B) 3D structure of the PG headgroup produced by our MD simulations. (C) 3D structure of the PG headgroup resulted from the quantum chemistry calculations. For clarity of presentation, hydrogen atoms are not shown except for the two hydroxyl oxygen atoms.

formed a strong intramolecular hydrogen bond (H-bond), which is geometrically unreasonable. The structure of the gel phase DPPG bilayer from experiment suggested that there should be no intramolecular H-bond between these two atoms.<sup>35</sup> In our simulations, all the atoms of POPG are described by the Berger force field. As a result, there is no H-bond formed between these two atoms in our simulation systems (Figure 1B). To further validate the results of our MD simulations, quantum chemical optimization was performed to obtain the low energy structure of POPG interacting with cations. The structure of the headgroup of POPG with a Na<sup>+</sup> ion was optimized by using the density functional theory method at the B3LYP/6-31G\* level. The resulting structure also shows that atom H6 does not form a H-bond with O8 (Figure 1C). A recent MD simulation using the CHARMM force field produced a structure of POPG similar to that in our simulations.<sup>35</sup> Accordingly, the structure of POPG without intramolecular H-bond between atoms H6 and O8 is suggested to be more reasonable than the one with a H-bond.

**Locations of Ions.** The locations of ions after long time equilibrium in the seven simulation systems were measured by atom density calculations (Figure 2). Used as a reference, the location of the phosphorus atom is also shown in Figure 2. The last snapshot of the MD trajectory for each system is shown in Figure 3 to give a direct view of ion distribution.

As can be seen in Figures 2 and 3, most of cations are located in or near the region of water/lipid interface in systems PG<sub>Na</sub> and PG<sub>K</sub>. Surprisingly, all of the 64 Ca<sup>2+</sup> ions in system PG<sub>Ca</sub> are entirely buried into the headgroup layer of the POPG bilayer. Moreover, most of the additionally added Ca<sup>2+</sup> ions are also located in the headgroup layer in system PG<sub>CaCl<sub>2</sub></sub> (Figure 3E). However, the additional 26 Na<sup>+</sup> ions in the system PG<sub>NaCl</sub> are all located far away from the headgroups of the lipids since there are already some Na<sup>+</sup> ions sparsely floating in bulk water in the simulation system

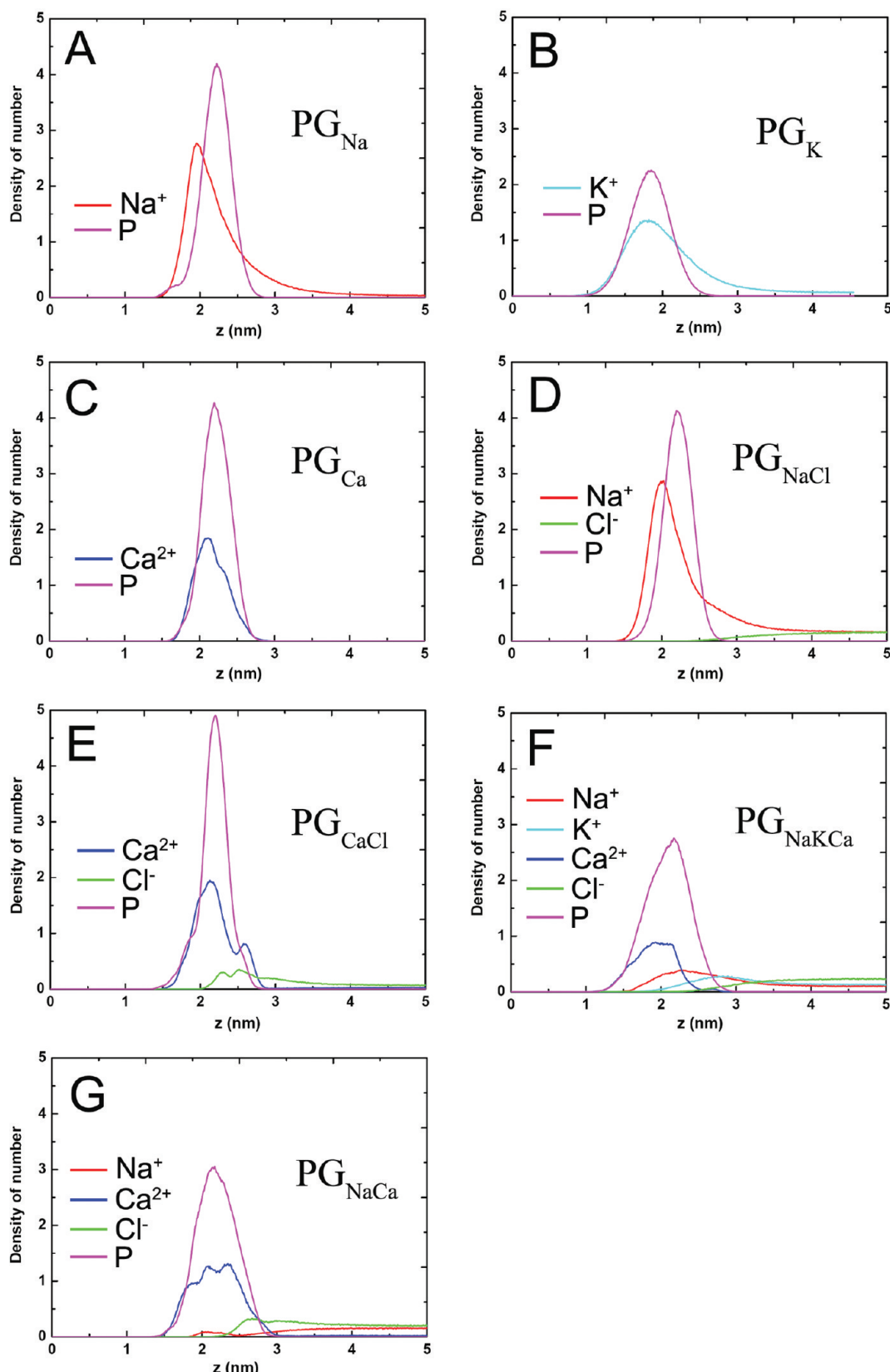


**Figure 2.** Density distributions of ions and phosphorus atom as a function of distance from the bilayer center ( $z = 0$ ) for seven simulation systems.

of  $\text{PG}_{\text{Na}}$  (Figure 2D,E). For system  $\text{PG}_{\text{NaKCa}}$  with the mixture of 80  $\text{Na}^+$ , 80  $\text{K}^+$ , and 40  $\text{Ca}^{2+}$  ions, all  $\text{Ca}^{2+}$  ions, a few  $\text{Na}^+$  ions, and fewer  $\text{K}^+$  ions are placed within the water/membrane interface region (Figures 2F and 3F). In system  $\text{PG}_{\text{NaCa}}$  where the number of  $\text{Ca}^{2+}$  ions is increased to 80,

more  $\text{Ca}^{2+}$  ions move to the water/membrane interface, and fewer  $\text{Na}^+$  ions stay in this region in comparison to those in the  $\text{PG}_{\text{NaKCa}}$  system (Figures 2G and 3G). This result indicates that  $\text{Ca}^{2+}$  has priority to abide within the water/membrane interface in comparison with  $\text{Na}^+$  and  $\text{K}^+$  ions.

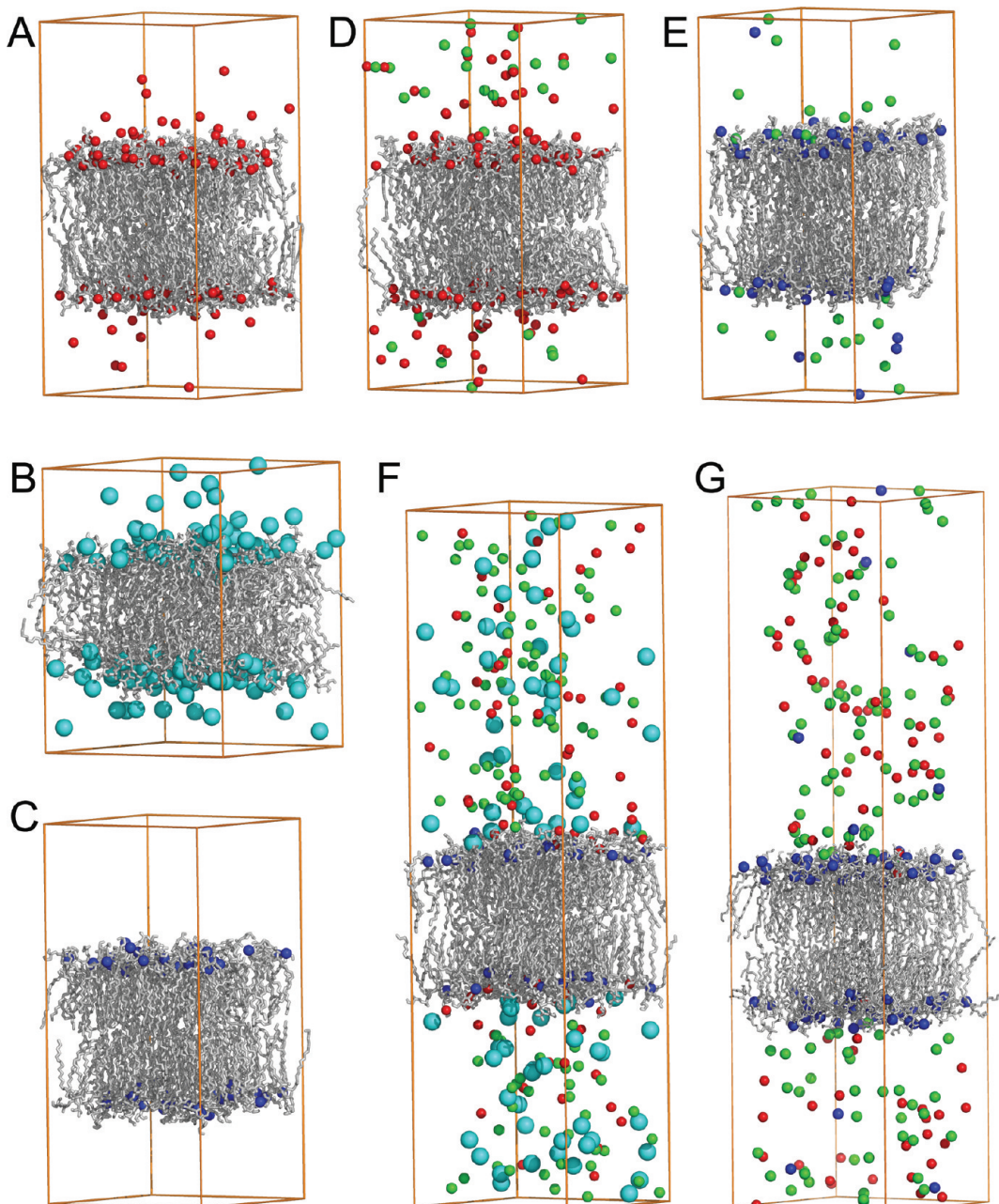


**Figure 3.** Last snapshot (without water molecules) of the trajectory for each of the seven simulation systems, PG<sub>Na</sub> (A), PG<sub>K</sub> (B), PG<sub>Ca</sub> (C), PG<sub>NaCl</sub> (D), PG<sub>CaCl<sub>2</sub></sub> (E), PG<sub>NaKCa</sub> (F), and PG<sub>NaCa</sub> (G). Na<sup>+</sup>, K<sup>+</sup>, Ca<sup>2+</sup>, and Cl<sup>-</sup> ions are displayed as red, cyan, blue, and green balls, respectively. Lipids are shown as gray sticks, and the unit cell is represented by orange lines.

**Area per Lipid.** The area per lipid ( $A_{\text{lipid}}$ ) is an important parameter to describe the structural properties of the lipid bilayer, since it represents the level of shrinking or swelling of the lipid bilayer. As shown in Table 1, the POPG bilayer in system PG<sub>K</sub> has the largest  $A_{\text{lipid}}$  value of  $\sim 68.2 \text{ \AA}^2$ . Differently, Na<sup>+</sup> and Ca<sup>2+</sup> counterions in PG<sub>Na</sub> and PG<sub>Ca</sub> remarkably reduce the value of  $A_{\text{lipid}}$  to  $\sim 51.0$  and  $\sim 50.6 \text{ \AA}^2$ , respectively. Therefore, the effects of different counterions on the area per lipid of POPG are in the following order: Ca<sup>2+</sup>  $\approx$  Na<sup>+</sup>  $>$  K<sup>+</sup>.

The  $A_{\text{lipid}}$  value of POPG in the PG<sub>NaCl</sub> system is  $\sim 51.4 \text{ \AA}^2$ , which is similar to that of PG<sub>Na</sub>, while it is reduced to  $\sim 49.4 \text{ \AA}^2$  in system PG<sub>CaCl<sub>2</sub></sub> because of the interactions of the 26 extra Ca<sup>2+</sup> ions. For the two systems with a mixture of ions, PG<sub>NaKCa</sub> and PG<sub>NaCa</sub>, lower  $A_{\text{lipid}}$  values of 50.4 and 49.3  $\text{\AA}^2$ , respectively, have been obtained for POPG. In summary, the largest  $A_{\text{lipid}}$  have been seen in system PG<sub>K</sub> and the systems including Ca<sup>2+</sup>

ions usually have a lower value of  $A_{\text{lipid}}$ . Moreover, the  $A_{\text{lipid}}$  could be further reduced by adding more Ca<sup>2+</sup> ions (e.g., in systems PG<sub>CaCl<sub>2</sub></sub> and PG<sub>NaCa</sub>, which contain 77 and 80 Ca<sup>2+</sup> ions, respectively). This indicates that Ca<sup>2+</sup> ions have a dominant role in affecting the area per lipid of POPG bilayer. It is also noticed that adding more Na<sup>+</sup> ions to the lipid bilayer does not have evident effects on the area per lipid because the values of  $A_{\text{lipid}}$  for POPG in PG<sub>Na</sub> and PG<sub>NaCl</sub> are very close (Table 2).

**Orientation of POPG Headgroup.** The binding of cations may affect the orientation of the PG headgroup due to the strong electrostatic interactions between the cations and the negative charge of POPG. The orientation of the PG headgroup is monitored by calculating the angle ( $\theta$ ) between the P-C4 vector and the outward normal axis of bilayer (Figure 4A). This angle can be used to reflect whether the PG headgroups are parallel or vertical to the membrane surface. For example, an angle of

**TABLE 2: Average Number of Oxygen Atoms per Ion in the First Coordination Shell of Cations**

system	O10	O11	O17	O38	water
PG <sub>Na</sub>	0.44	0.56	0.85	0.53	2.93
PG <sub>K</sub>	0.18	0.22	0.26	0.19	5.61
PG <sub>Ca</sub>	1.34	1.40	1.62	0.11	2.68
PG <sub>NaCl</sub>	0.36	0.42	0.69	0.43	3.38
PG <sub>CaCl<sub>2</sub></sub>	1.23	1.29	1.40	0.12	3.02
PG <sub>NaKC<sub>a</sub></sub> (Na)	0.07	0.11	0.21	0.11	4.81
PG <sub>NaKC<sub>a</sub></sub> (K)	0.01	0.02	0.01	0.02	6.32
PG <sub>NaKC<sub>a</sub></sub> (Ca)	1.53	1.70	2.12	0.19	1.37
PG <sub>NaCa</sub> (Na)	0.02	0.03	0.11	0.01	5.15
PG <sub>NaCa</sub> (Ca)	1.13	1.23	1.29	0.12	3.36

~90° means the PG headgroup is almost parallel to the membrane surface.

The distribution probability as well as the average value of  $\theta$  for each system is presented in Figure 4B. The  $\theta$ -probability curves for the seven simulation systems can be divided into three groups according to the locations of curve peaks and the average values of  $\theta$ . PG<sub>K</sub> can be catalogued into the first group with a peak at ~105° and the largest averaged  $\theta$  of ~94.5°. These two data indicate that the PG headgroups in system PG<sub>K</sub> are on average parallel to the membrane surface. This result also interprets the larger  $A_{\text{lipid}}$  of POPG in this system. The second group includes the two systems, PG<sub>Na</sub> and PG<sub>NaCl</sub>. Their curve peaks are both around  $\theta \approx 70^\circ$  and their average values of  $\theta$  are 74.5° and 73.0°, respectively, suggesting that Na<sup>+</sup> ions make the headgroups more vertical to the membrane surface than K<sup>+</sup> ions do. The third group is associated with the systems involving Ca<sup>2+</sup> ions, i.e., PG<sub>Ca</sub>, PG<sub>CaCl<sub>2</sub></sub>, PG<sub>NaKC<sub>a</sub></sub>, and PG<sub>NaCa</sub>. The average  $\theta$  values for systems PG<sub>Ca</sub>, PG<sub>CaCl<sub>2</sub></sub>, PG<sub>NaKC<sub>a</sub></sub>, and PG<sub>NaCa</sub> are 67.2°, 66.1°, 71.1°, and 64.8°, respectively, which are even smaller than those of PG<sub>Na</sub> and PG<sub>NaCl</sub>. It is thus indicated that the POPG headgroups in these systems are more vertical to the membrane surface than those of other systems without Ca<sup>2+</sup> ions. Moreover, more Ca<sup>2+</sup> ions results in smaller  $\theta$ , suggesting more Ca<sup>2+</sup> ions have a stronger effect on the structural changes of the bilayer.

It should be emphasized that there is a good correlation between the area per lipid and the headgroup orientation. In system PG<sub>K</sub> the PG headgroups are almost parallel to the membrane surface and thus occupy more space, resulting in the largest  $A_{\text{lipid}}$  among the seven systems. When Na<sup>+</sup> ions are bound to lipids, the PG headgroups stick to the membrane surface,

resulting in a smaller  $A_{\text{lipid}}$  value. The  $A_{\text{lipid}}$  values of PG<sub>NaCa</sub> and PG<sub>CaCl<sub>2</sub></sub> are the smallest among the seven systems, as their PG headgroups are the most vertical with respect to the membrane surface.

**Ordering of sn-1 and sn-2 Chains.** The ordering of the two hydrophobic tails, sn-1 and sn-2 chains, of the lipid is characterized by the deuterium order parameter ( $S_{CD}$ ).<sup>51,52</sup> The  $S_{CD}$  values of sn-1 and sn-2 chains for all simulation systems are plotted in Figure 5. The  $S_{CD}$  values of sn-1 and sn-2 chains for POPG in systems PG<sub>K</sub> are significantly smaller than those of other six systems, suggesting that the acyl chains of POPG are most disordered in the bilayer with K<sup>+</sup> counterions. As mentioned above, the lipid bilayer with K<sup>+</sup> ions has a larger  $A_{\text{lipid}}$  value, which provides more spaces for the motions of acyl chains and thus results in the smaller  $S_{CD}$  parameter. Similar to the  $A_{\text{lipid}}$  values, the  $S_{CD}$  parameters for PG<sub>Na</sub> and PG<sub>Ca</sub> are also quite close.

The ordering of sn-2 chains in systems PG<sub>Na</sub> and PG<sub>NaCl</sub> are similar, but the sn-1 chains in PG<sub>NaCl</sub> are relative less ordered than that in PG<sub>Na</sub>. The excess of Na<sup>+</sup> ions slightly decreases the ordering of the hydrocarbon chains. However, the additional Ca<sup>2+</sup> ions lead the sn-1 and sn-2 chains to be in a more ordered state as the  $S_{CD}$  values of both sn-1 and sn-2 chains in PG<sub>CaCl<sub>2</sub></sub> are higher than those in PG<sub>Ca</sub>. It is consistent with the results of other parameters that more Ca<sup>2+</sup> ions bring a stronger effect on the structure of the lipid bilayer.

The ordering of acyl chains in systems PG<sub>NaKC<sub>a</sub></sub> is similar to that in PG<sub>Na</sub> and PG<sub>Ca</sub>. In comparison with PG<sub>NaKC<sub>a</sub></sub>, the increased Ca<sup>2+</sup> ions in PG<sub>NaCa</sub> increase the ordering of sn-1 and sn-2 chains. However,  $S_{CD}$  values for POPG in PG<sub>NaCa</sub> are smaller than those in PG<sub>CaCl<sub>2</sub></sub>, although both systems contain similar Ca<sup>2+</sup> ions. It may be caused by the extra Na<sup>+</sup> and Cl<sup>-</sup> ions in system of PG<sub>NaCa</sub>. A similar observation has been found for PG<sub>Na</sub> and PG<sub>NaCl</sub> that the additional Na<sup>+</sup> and Cl<sup>-</sup> ions in PG<sub>NaCl</sub> caused the two acyl chains less ordered.

**Ion–Lipid Interactions.** Ion–lipid interaction is a key factor to maintain the stability of lipid bilayers, in particular, for the lipid bilayers composed of anionic lipids. Therefore, we analyzed the ion–lipid interactions for all seven systems by calculating three parameters, i.e., numbers of oxygen atoms interacting with a cation within its first coordination shell, bound ions and ion–lipid bonds. The results are listed in Tables 2–4. The probabilities of four oxygen atoms (O10, O11, O17, and O38 in Figure 1A) as well as oxygen atoms in water molecules located within the first coordination shell of each cation were

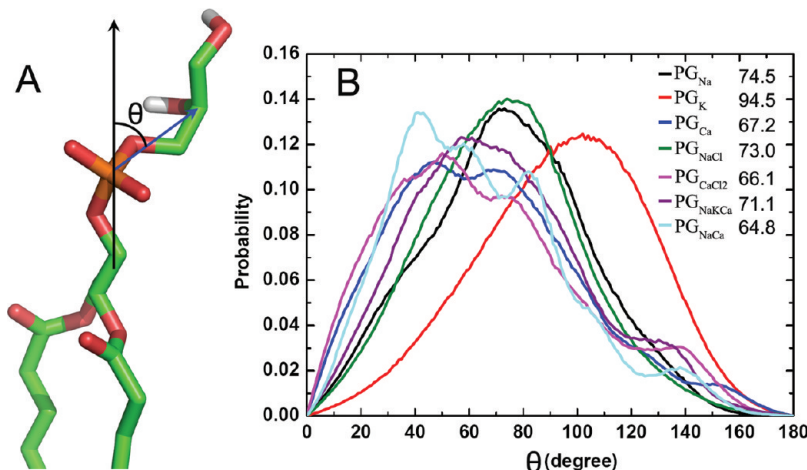


**Figure 4.** (A) Orientation of the PG headgroup described by the angle ( $\theta$ ) between the P→C4 vector (blue arrow) and the outward bilayer normal (black arrow). (B) Probability distribution of  $\theta$ . The average value of the angle for each system is listed in the top right corner of the plots.

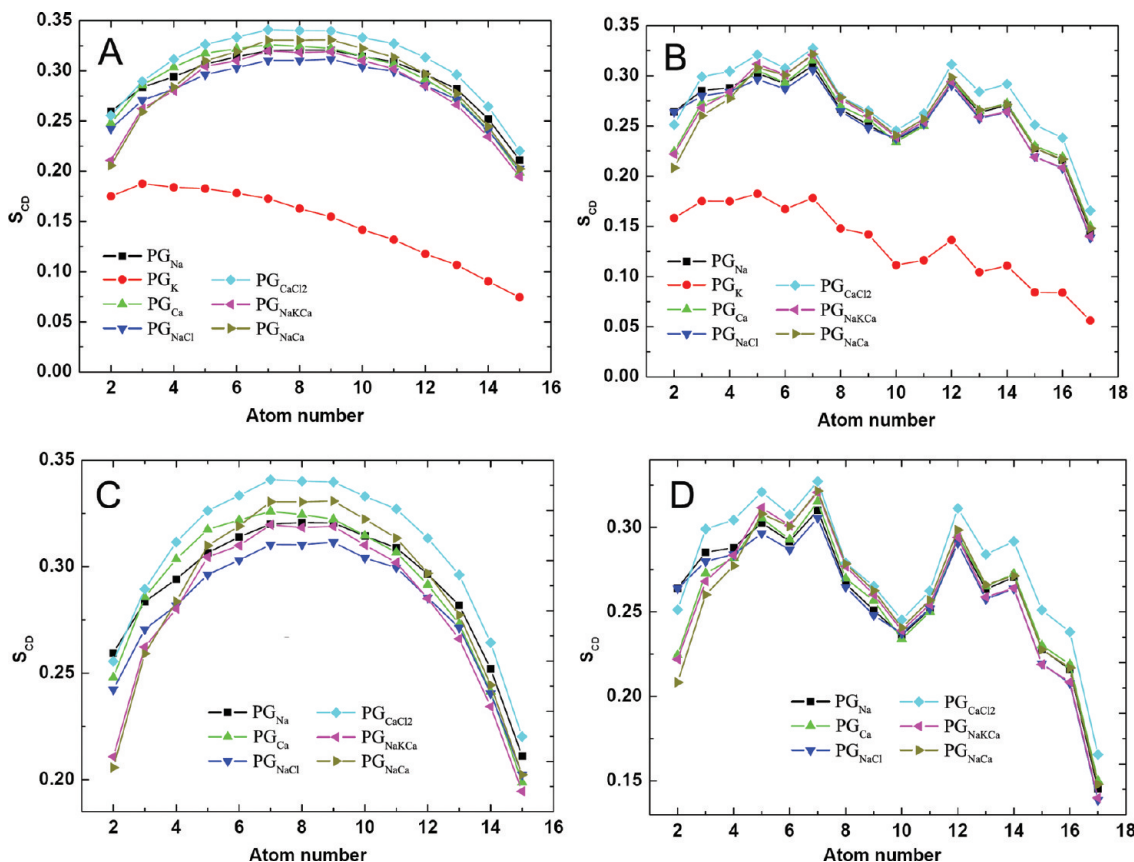


**Figure 5.** Deuterium order parameter ( $S_{CD}$ ) of *sn*-1 (A) and *sn*-2 (B) chains of POPG in seven simulation systems. (C) and (D) are the enlarged view of the top six curves in (A) and (B), respectively.

**TABLE 3: Average Number of Ions Binding to None, One, Two, Four, or Five Lipids**

system	none	one	two	three	four	five
PG <sub>Na</sub>	30.6	14.6	21.6	32.6	26.2	2.3
PG <sub>K</sub>	66.7	32.3	19.4	8.0	1.5	0.1
PG <sub>Ca</sub>	0.0	1.2	8.5	23.9	27.8	2.5
PG <sub>NaCl</sub>	55.2	17.2	23.4	33.2	22.5	2.5
PG <sub>CaCl<sub>2</sub></sub>	4.5	2.5	12.5	29.8	22.2	5.5
PG <sub>NaKCa</sub> (Na)	63.6	5.4	4.5	5.2	1.3	0.0
PG <sub>NaKCa</sub> (K)	76.8	1.9	0.8	0.4	0.1	0.0
PG <sub>NaKCa</sub> (Ca)	0.0	0.0	0.2	6.9	27.0	5.9
PG <sub>NaCa</sub> (Na)	76.6	0.3	0.1	2.4	0.6	0.0
PG <sub>NaCa</sub> (Ca)	10.5	3.9	17.0	13.9	28.5	6.1

**TABLE 4: Average Number of Ion–Lipid Bonds**

system	ion–O10	ion–O11	ion–O17	ion–O38
PG <sub>Na</sub>	55.9	72.1	108.4	67.6
PG <sub>K</sub>	22.8	28.1	33.4	24.6
PG <sub>Ca</sub>	85.9	89.4	103.7	6.8
PG <sub>NaCl</sub>	55.3	64.3	106.9	66.2
PG <sub>CaCl<sub>2</sub></sub>	94.5	99.1	107.4	9.4
PG <sub>NaKCa</sub> (Na)	5.7	8.9	16.5	8.6
PG <sub>NaKCa</sub> (K)	1.0	1.2	0.9	1.7
PG <sub>NaKCa</sub> (Ca)	61.1	68.3	85.0	7.7
PG <sub>NaCa</sub> (Na)	1.4	2.4	8.6	1.1
PG <sub>NaCa</sub> (Ca)	90.2	98.2	103.4	9.6

measured by calculating the radial distribution function (rdf) between the ion and the oxygen atoms and then integrating the distribution profile from zero to a cutoff distance.<sup>22</sup> The cutoff distances of Na<sup>+</sup>, K<sup>+</sup>, and Ca<sup>2+</sup> ions are 0.31, 0.36, and 0.30 Å, respectively.<sup>22</sup> An ion with a distance to any of the four lipid oxygens less than the cutoff distance was considered a bound ion. The numbers of ions binding to none, one, two, three, four,

and five lipids in each system were also calculated. We define an ion–lipid bond as formed when the distance of the oxygen atom to an ion is smaller than the cutoff distance.<sup>34</sup>

The ion–lipid interactions in the systems with pure counterions reflect the intrinsic properties of the binding between the ions and lipids. Such ion–lipid interactions were thus first analyzed for systems PG<sub>Na</sub>, PG<sub>K</sub>, and PG<sub>Ca</sub>. Obviously, most of the K<sup>+</sup> ions coordinate with water molecules (Table 2), and only a small portion of K<sup>+</sup> ions could interact with the four kinds of oxygen atoms of POPG molecules. This is different from the simulation result on neutral lipids, which indicated that all K<sup>+</sup> ions interact with water molecules rather than with the lipids.<sup>20,22</sup> For PG<sub>Na</sub> and PG<sub>Ca</sub>, more lipid oxygens appear in the first coordination shell of counterions (Table 2), indicating that more Na<sup>+</sup> and Ca<sup>2+</sup> ions interact directly with the lipid molecules. Figure 6 show two typical snapshots of Na<sup>+</sup> and Ca<sup>2+</sup> ions coordinating with lipid oxygens. There are differences among the coordination patterns for Na<sup>+</sup>, K<sup>+</sup>, and Ca<sup>2+</sup> ions with the oxygens of lipids. Na<sup>+</sup> or K<sup>+</sup> usually coordinates with four oxygens (O10, O11, O17, and O38), while Ca<sup>2+</sup> strongly interacts with three of them (O10, O11, and O17) (Table 2 and Figure 6). Na<sup>+</sup> or K<sup>+</sup> almost equally coordinate with the carbonyl oxygen atoms from each of the two chains of POPG (O17 and O38), whereas Ca<sup>2+</sup> favors to coordinate with the carbonyl oxygen atom in *sn*-2 chains (O17) (Table 2). Further analysis revealed that about 66 of the 128 K<sup>+</sup> counterions in PG<sub>K</sub> and 30 of the 128 Na<sup>+</sup> counterions in PG<sub>Na</sub> do not interact with lipids, but all 64 Ca<sup>2+</sup> counterions in PG<sub>Ca</sub> are bound to lipids (Table 3). While the major bound K<sup>+</sup> counterions interact with either one or two lipids, most of the bound Ca<sup>2+</sup> ions coordinate with three or four lipids (Figure 6). For the bound Na<sup>+</sup> counterions, there is no obverse difference among the

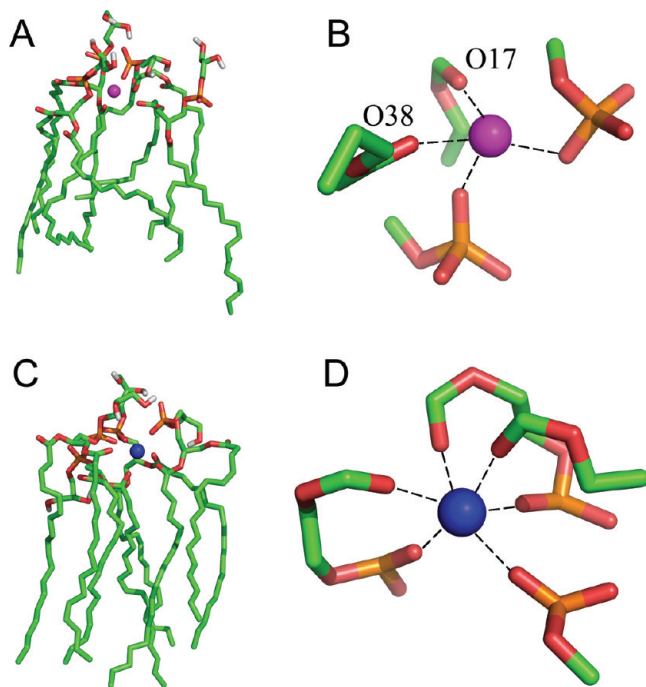


**Figure 6.** Typical snapshots of  $\text{Na}^+$  and  $\text{Ca}^{2+}$  ions coordinating with lipid oxygen atoms.  $\text{Na}^+$  and  $\text{Ca}^{2+}$  ions are displayed in magenta and blue balls, respectively. Lipids are represented by sticks. The dashed lines indicate the coordination bond. (A) 3D structure of  $\text{Na}^+$  ion coordinating with adjacent lipids. (B) Close view of the coordination pattern of the  $\text{Na}^+$  ion with O17 and O38, and two phosphate oxygens. (C) 3D structure of  $\text{Ca}^{2+}$  ion coordinating with adjacent lipids. (D) Close view of the coordination pattern of  $\text{Ca}^{2+}$  ion with three O38 atoms and three phosphate oxygens.

number of ions that coordinate with one, two, three, and four lipids. Only two  $\text{Na}^+$  ions interact with five lipids simultaneously. Finally, the ion–lipid bonds are consistent with the numbers of oxygens per cation in the first coordination shell.  $\text{K}^+$  ions formed few ion–lipid bonds with four oxygens (O10, O11, O17, and O38) in system PG<sub>K</sub> (Tables 2 and 4). In contrast, ions formed much more ion–lipid bonds in systems PG<sub>Na</sub> and PG<sub>Ca</sub>. All the ion–O10, ion–O11, ion–O17, and ion–O38 bonds are abundant in PG<sub>Na</sub> (Tables 2 and 4). Interestingly, most of the ion–lipid bonds in system PG<sub>Ca</sub> are formed between  $\text{Ca}^{2+}$  ions and atoms O10, O11, and O17, only a few are ion–O38 bonds (Tables 2 and 4).

It is found that the number of ions that do not bind to any lipid is increased from 30.6 in PG<sub>Na</sub> to 55.2 in PG<sub>NaCl</sub> (Table 3). This indicates that the additionally added  $\text{Na}^+$  ions in PG<sub>NaCl</sub> do not interact with lipids. In fact, the total ion–lipid bonds in PG<sub>NaCl</sub> are even slightly less than that in PG<sub>Na</sub>. As a result, the additional  $\text{Na}^+$  ions do not increase the ion effects on the structure of POPG bilayer as discussed above. Different from  $\text{Na}^+$  ions, most of the additional  $\text{Ca}^{2+}$  ions in PG<sub>CaCl<sub>2</sub></sub> are bound to lipids (Table 3). Consequently, there are more ion–lipid bonds in PG<sub>CaCl<sub>2</sub></sub>.  $\text{Ca}^{2+}$  ions in PG<sub>CaCl<sub>2</sub></sub> form  $\sim 310$  ion–lipid bonds, and more than the 286 ion–lipid bonds in PG<sub>Ca</sub> (Table 3). This result explains why the POPG lipids have smaller  $A_{\text{lipid}}$  values and greater  $S_{\text{CD}}$  parameters in PG<sub>CaCl<sub>2</sub></sub> than in PG<sub>Ca</sub>; i.e., the strong  $\text{Ca}^{2+}$ –lipid interactions tighten up the lipid molecules.

In PG<sub>NaKCa</sub>,  $\text{Ca}^{2+}$  ions interact with atoms O10, O11, and O17 with coordination numbers 1.53, 1.70, and 2.12, respectively, which are larger than the corresponding numbers in PG<sub>Ca</sub> (Table 2). The 40  $\text{Ca}^{2+}$  ions in PG<sub>NaKCa</sub> form 219 ion–lipid bonds (Table 4) and the average coordination number for each  $\text{Ca}^{2+}$  ion is  $\sim 5.5$ . In contrast to the increased binding of  $\text{Ca}^{2+}$  ions

with lipids,  $\text{Na}^+$  and  $\text{K}^+$  ions show decreased binding with lipids in PG<sub>NaKCa</sub>. The average number of lipid oxygens per  $\text{K}^+$  ion in the first coordination shell is quite low (Table 2). Actually, as shown in Figures 2B and 3B, almost all  $\text{K}^+$  ions are far from the bilayer surface. The average numbers of oxygen atoms per  $\text{Na}^+$  in the first coordination shell also decreased dramatically in PG<sub>NaKCa</sub>, compared with those in PG<sub>Na</sub> (Table 2). The 80  $\text{Na}^+$  ions in PG<sub>NaKCa</sub> only form 39 ion–lipid bonds (Table 4). About 64 of the 80  $\text{Na}^+$  ions do not bind with any lipid (Table 3). Therefore, the binding ability to the lipids for the three cations is in the order of  $\text{Ca}^{2+} > \text{Na}^+ > \text{K}^+$ . Moreover,  $\text{Ca}^{2+}$  ions show the ability to inhibit the binding of  $\text{Na}^+$  and  $\text{K}^+$  ions to lipids. The simulation result from PG<sub>NaCa</sub> suggests that the increased  $\text{Ca}^{2+}$  ions could further inhibit the binding of  $\text{Na}^+$  ions to lipids. Almost no lipid oxygen is in the first coordination shell of  $\text{Na}^+$  ions in PG<sub>NaCa</sub> (Table 2), and only  $\sim 3$   $\text{Na}^+$  ions are bound to lipids in PG<sub>NaCa</sub>, while about 16  $\text{Na}^+$  ions are bound to lipids in PG<sub>NaKCa</sub> (Table 3). Accordingly, the 120  $\text{Na}^+$  ions formed few ion–lipid bonds in system PG<sub>NaCa</sub> (Table 4).

## Discussion

**Long-Time Simulation Is Necessary to Study Cation Effects on POPG Bilayer.** On the basis of 40–60 ns MD simulations, Pedersen et al. concluded that  $\text{Ca}^{2+}$  counterions have a more pronounced effect than  $\text{Na}^+$  counterions on the area per lipid of anionic DMPS.<sup>32</sup> In the present study,  $\mu\text{s}$ -MD simulations have been performed on the POPG lipid bilayer neutralized by  $\text{K}^+$ ,  $\text{Na}^+$ , and  $\text{Ca}^{2+}$  ions in the water solution. Indeed, our simulations indicate that the lipids in PG<sub>Na</sub> have a larger area per lipid than those in PG<sub>Ca</sub> during the first 50 ns (Figure 7). It seems that  $\text{Ca}^{2+}$  ions may have a stronger influence on the lipid structure, which is consistent with the conclusion from the short-time simulations.<sup>32</sup> Nevertheless, when the simulations continue, the curves of the areas per lipid of these two systems versus simulation time come together. After  $\sim 0.25 \mu\text{s}$ , the two trajectories converge to and fluctuate around  $50 \text{ \AA}^2$ . This result indicates that there is no pronounced difference between the effects of  $\text{Na}^+$  and  $\text{Ca}^{2+}$  ions on the area per lipid of the POPG bilayer when the ions are added as counterions. Also, our simulations suggest that  $\text{Ca}^{2+}$  ions may quickly stabilize the POPG bilayer, after  $\sim 120$  ns the area per lipid is converged, but the structure of the POPG bilayer is not stabilized by  $\text{Na}^+$  ions until  $\sim 250$  ns (Figure 7A). This possibly is the reason why the short-time simulations gave a false appearance that  $\text{Ca}^{2+}$  counterions have a more pronounced effect than  $\text{Na}^+$  counterions on the area per lipid of charged lipid bilayer.<sup>32</sup> Overall, our simulation results indicate that long-time effects of ions on lipid bilayer structures should exist, and thereby long-time simulations are necessary to address such effects, while short-time simulations may cause artificial results.

**Effects of  $\text{K}^+$ ,  $\text{Na}^+$ , and  $\text{Ca}^{2+}$  as Counterions on the POPG Bilayer.** Although no profound difference between the effects of  $\text{Ca}^{2+}$  and  $\text{Na}^+$  on the area per lipid has been observed when these ions act as counterions, our long-time MD simulations indeed addressed the difference for the action effect of  $\text{K}^+$  ions with respect to those of  $\text{Ca}^{2+}$  and  $\text{Na}^+$  ions on the POPG bilayer structure. In comparison with  $\text{Ca}^{2+}$  and  $\text{Na}^+$  ions,  $\text{K}^+$  ions almost have no effect on the area per lipid of POPG bilayer (Figure 7) which fluctuates around  $67 \text{ \AA}^2$ . The change tendency for the area per lipid is in agreement with other parameters such as ion–lipid interaction, headgroup orientation, and ordering of *sn*-1 and *sn*-2 chains. Ion–lipid interaction analysis illustrates that  $\text{Ca}^{2+}$  and  $\text{Na}^+$  ions interact more strongly than  $\text{K}^+$  ions with POPG lipids, as indicated by the numbers of lipid oxygens

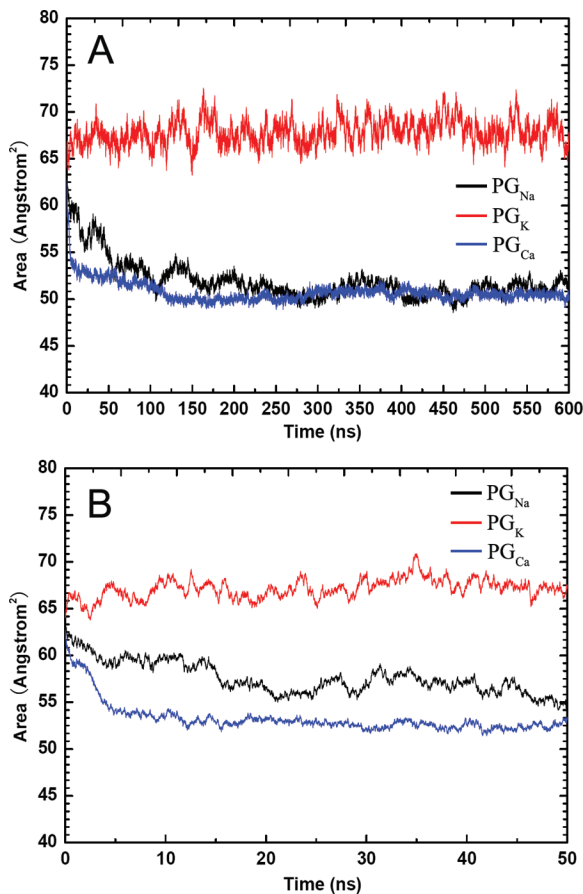


**Figure 7.** (A) Area per lipid as a function of simulation time for POPG bilayers in the trajectories of the three simulation systems, PG<sub>Na</sub>, PG<sub>K</sub>, and PG<sub>Ca</sub>. (B) Enlarged view of the first 50 ns of the three trajectories represented in (A).

interacting with a cation within its first coordination shell (Table 2), bound ions (Table 3), and ion–lipid bonds (Table 4). In particular, only a small portion of K<sup>+</sup> ions directly bond with the lipid molecules (Tables 2 and 3, Figure 3B). In principle, the stronger interactions of Ca<sup>2+</sup> and Na<sup>+</sup> ions induce the headgroups of the lipid molecules to be more vertical with respect to the membrane surface, as indicated by the calculated  $\theta$  angles (Figure 4). The vertical headgroups of POPG lipids bound by Ca<sup>2+</sup> or Na<sup>+</sup> ions occupy less space, producing small  $A_{\text{lipid}}$  values in comparison with those for the POPG lipids bound with K<sup>+</sup> ions (Table 1). In comparison with the headgroups parallel to the membrane surface (e.g., the headgroup of the lipids in pure POPG bilayers or bilayers bound by K<sup>+</sup> ions), the vertical headgroups of lipids may also adopt a tighter arrangement, which further imposes restriction on the motions of the *sn*-1 and *sn*-2 chains of lipid molecules. Indeed, the  $S_{\text{CD}}$  values of the two chains in PG<sub>Ca</sub> and PG<sub>Na</sub> systems are much higher than those in the PG<sub>K</sub> system (Figure 5A,B), indicating that the hydrophobic tails of lipids in PG<sub>Ca</sub> and PG<sub>Na</sub> systems are more ordered. All these data demonstrated that Ca<sup>2+</sup> and Na<sup>+</sup> impact the membrane structure more dramatically than K<sup>+</sup> do, implying that K<sup>+</sup> performs its biological functions mostly through direct interactions with membrane proteins (e.g., ion channels), whereas Ca<sup>2+</sup> and Na<sup>+</sup> may bring in biological effects by regulating the membrane structures in addition to direct binding to membrane proteins (see discussion below).

**Extra Ca<sup>2+</sup> Ions Result in Stronger Effects While Extra Na<sup>+</sup> Ions Do Not.** Encouraged by the study of the effects of K<sup>+</sup>, Na<sup>+</sup>, and Ca<sup>2+</sup> as counterions on the structure of POPG

bilayer, we investigated the effects of how extra ions affect the structures of lipid bilayers. As expected, additional K<sup>+</sup> ions have no further effect on the structure of the POPG bilayer (data not shown). Different from the effects of counterions, extra Na<sup>+</sup> and Ca<sup>2+</sup> ions display different performances on the structure of the POPG bilayer. Most of the 26 additional Ca<sup>2+</sup> ions in PG<sub>CaCl<sub>2</sub></sub> are bound to lipids, and the total number of bound Ca<sup>2+</sup> ions to the bilayer reaches  $\sim$ 72 (Table 3), thereby producing more ion–lipid bonds than the PG<sub>Ca</sub> system (Table 4). As a consequence, for system PG<sub>CaCl<sub>2</sub></sub> the  $A_{\text{lipid}}$  value is further reduced (Table 1), the orientation of headgroups is more vertical to the membrane surface of the bilayer, and the acyl chains are more ordered (Figures 4 and 5B). Nevertheless, the extra Na<sup>+</sup> ions do not produce any more effect on the structure of the POPG bilayer in system PG<sub>NaCl</sub>, as indicated by the calculated parameters of the  $A_{\text{lipid}}$  value (Table 1), the number of bound ions (Table 3) and ion–lipid bonds (Table 4), headgroup orientation (Figure 4), and the orderings of headgroups and acyl chains (Figure 5). This finding suggests that, although no profoundly different effects have been observed when Na<sup>+</sup> and Ca<sup>2+</sup> ions are both applied to the POPG bilayer as counterions, Ca<sup>2+</sup> ions show distinct effects on the POPG bilayer structure when extra ions are added to the bilayer; i.e., the extra Ca<sup>2+</sup> ions further influence the POPG bilayer by stabilizing and tightening the structure of the bilayer (Tables 1–4 and Figure 4). This result implies that, in biological systems, Ca<sup>2+</sup> may regulate the functions of some membranes or membrane proteins by changing its concentration, as will be discussed below.

**Ca<sup>2+</sup> Ions in the Ion Mixture Display Dominative Effects on the Structure of the POPG Bilayer.** As has been discussed above, Ca<sup>2+</sup> ions behave a unique role in affecting the structure of the POPG bilayer. To further address the special role of Ca<sup>2+</sup> ions in affecting the lipid bilayer structure, we designed two simulation systems composed of a POPG bilayer and multiple ions including Na<sup>+</sup>, K<sup>+</sup>, and Ca<sup>2+</sup> ions, on which two  $\mu$ s-MD simulations were performed, respectively. The MD simulation result for system PG<sub>NaKC<sub>a</sub></sub> consisting of the POPG bilayer, 80 Na<sup>+</sup> ions, 80 K<sup>+</sup> ions, and 40 Ca<sup>2+</sup> ions demonstrated that most of the ion–lipid bonds were formed between Ca<sup>2+</sup> ions and lipids rather than between Na<sup>+</sup> or K<sup>+</sup> and lipids, although the number of Ca<sup>2+</sup> ions is only half of that for Na<sup>+</sup> or K<sup>+</sup> ions in PG<sub>NaKC<sub>a</sub></sub>. So, consistent with experimental results,<sup>53,54</sup> our MD simulations also suggested that the Ca<sup>2+</sup> ion binds more strongly with anionic lipids than K<sup>+</sup> and Na<sup>+</sup> ions do. Among the mixture of ions, all 40 Ca<sup>2+</sup> ions are bound to lipids while most Na<sup>+</sup> ions and almost all K<sup>+</sup> ions do not interact with lipids (Table 3). Therefore, the binding of Na<sup>+</sup> and K<sup>+</sup> ions to lipids is greatly inhibited by Ca<sup>2+</sup> ions. As a result, the structure of the POPG bilayer is most influenced by Ca<sup>2+</sup> ions. The MD simulation result from the second system PG<sub>NaCa</sub> that is composed of the POPG bilayer, 80 Na<sup>+</sup> ions, and 80 Ca<sup>2+</sup> ions illustrated that binding of Na<sup>+</sup> ions to the lipids was further inhibited by the increased Ca<sup>2+</sup> ions. Almost no Na<sup>+</sup> ion is bound to POPG in system PG<sub>NaCa</sub> (Table 3). The  $A_{\text{lipid}}$  values and the ordering of the lipid chains also indicated that Ca<sup>2+</sup> ions of the ion mixture dominated the effects of the ions on the structure of the POPG bilayer (Table 1 and Figure 5B).

In a physiological environment, the ion composition is very complex and usually multiple cations, such as Na<sup>+</sup>, K<sup>+</sup>, and Ca<sup>2+</sup>, coexist around a patch of membrane (e.g., lipid raft). Previous simulations have only widely studied the effects of Na<sup>+</sup> ions on some lipid bilayers, and few have studied the effects of other ions on neutral lipid bilayers.<sup>16–24,55</sup> The effects of an

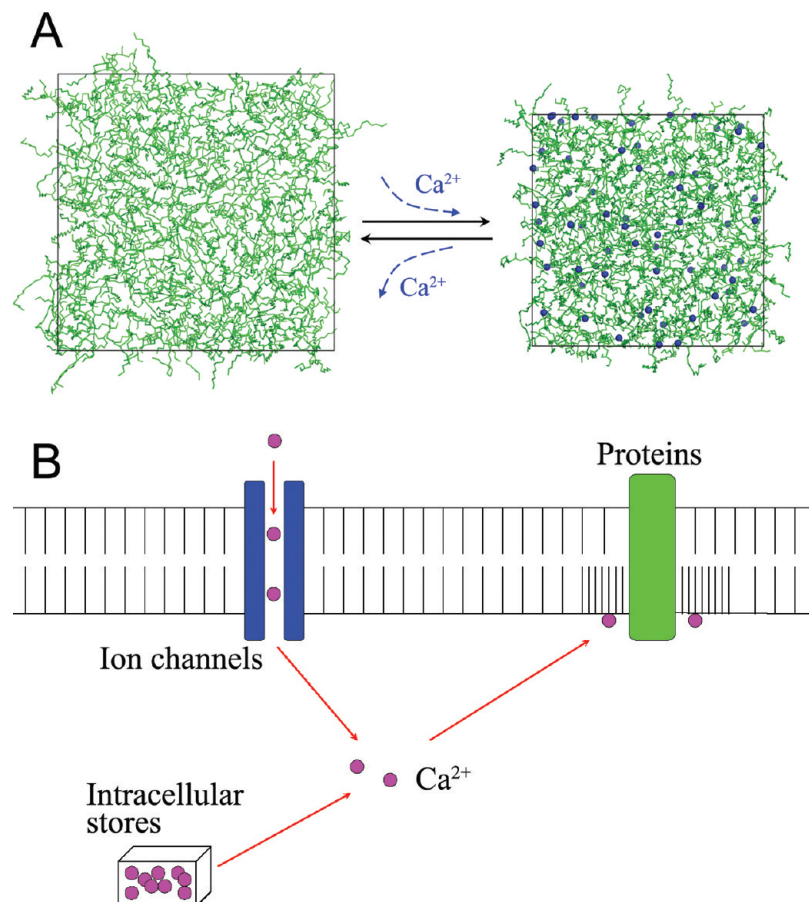


**Figure 8.** (A) Shrinking of the POPG bilayer caused by  $\text{Ca}^{2+}$  ions binding. The binding of  $\text{Ca}^{2+}$  ions leads to smaller area per lipid. Thus the changes of calcium concentration could result in mechanical movements of the cell membrane. Lipids are shown as green lines, and  $\text{Ca}^{2+}$  ions are displayed in blue balls. The unit cells are labeled by black lines. (B) Schematic representation of the functions of  $\text{Ca}^{2+}$  ions on membrane structures based on the simulation results. The changes of calcium concentration affect the structures and movements of cell membrane, such as swelling or shrinking, which may further mediate the functions of proteins that are membrane embedded or adhere to the membrane surface.  $\text{Ca}^{2+}$  ions are shown as magenta balls. The red arrows indicate the directions for the transport of  $\text{Ca}^{2+}$  ions.

ion mixture consisting of several ions such as  $\text{Na}^+$ ,  $\text{K}^+$ , and  $\text{Ca}^{2+}$  on membrane structures have not been investigated yet. Our MD simulations, for the first time, provide such a study and conclude that  $\text{Ca}^{2+}$  ions play a special role in regulating the structure of a membrane, which might be used to explain several biological functions of  $\text{Ca}^{2+}$  ions, as will be discussed below.

**Biological Implications of  $\text{Ca}^{2+}$  Effects on Anionic Lipids.**  $\text{Ca}^{2+}$  ions play important roles in biological systems. For example, as a second messenger, intracellular  $\text{Ca}^{2+}$  ions play fundamental roles in many signal transduction pathways. Most interestingly,  $\text{Ca}^{2+}$  ions may regulate biological processes not only by means of direct binding with proteins (e.g., calmodulins and some potassium ion channels) but also by regulating the structure of cell membranes.<sup>56–65</sup> Much attention has been paid to the direct regulation mechanisms of  $\text{Ca}^{2+}$  ions, which are generally associated with the conformational changes of  $\text{Ca}^{2+}$ -binding proteins. However, the regulation mechanisms of  $\text{Ca}^{2+}$  ions by affecting the membrane structures have not been appreciated. On the basis of the MD simulation results that calcium could dominantly affect the membrane structures, we propose a dynamic mechanism for this kind of regulation (Figure 8). By association with and dissociation from lipid molecules,  $\text{Ca}^{2+}$  ions may strongly affect the structures of the membrane, such as tightening and loosening the membrane, as shown in Figure 8A. The calcium concentration is regulated by many factors, including ion channels and intracellular stores. The

changes of calcium concentration might mediate the membrane structure, which may further regulate the permeability and mobility of the membranes, and the structures (conformations) and aggregations of embedded proteins as well (Figure 8B), helping the biological systems to accomplish functions such as signaling and apoptosis.

This mechanism addressed above may help to explain the regulation mechanisms of  $\text{Ca}^{2+}$  ions for some mechanosensitive channels. For instance, TRPA1 is a mechanosensitive channel that can be activated by  $\text{Ca}^{2+}$  ions.<sup>66,67</sup> Zurborg et al.<sup>66</sup> speculated that  $\text{Ca}^{2+}$  ions activate human TRPA1 via the direct binding of  $\text{Ca}^{2+}$  ions to the EF-hand domain. Here, we suggest an alternative mechanism that TRPA1 might be activated by the membrane mechanical motions caused by  $\text{Ca}^{2+}$  ion binding. *Drosophila* Painless, a member of the TRP ion channel superfamily, is a  $\text{Ca}^{2+}$ -requiring channel.<sup>68</sup> However, different from the human TRPA1, this channel does not have a  $\text{Ca}^{2+}$  ion binding site. As mentioned above, the  $\text{Ca}^{2+}$  ion may concentration dependently affect the lipid bilayer structure (Tables 1 and 4 and Figure 5). Consequently, the concentration changes of  $\text{Ca}^{2+}$  ions will lead to swelling or shrinking motions of the membrane, which further trigger the conformational changes of TRP ion channels. Interestingly, it is found that TRP channels are located within anionic lipid abundant membranes (the AOCS Lipid Library, <http://lipidlibrary.aco.org/>). Additionally, our MD simulation result also could be used to explain many biological mechanisms of other proteins such as annexin,<sup>62,64</sup> protein kinase

$C_\alpha$ ,<sup>63</sup> 15-lipoxygenase-1,<sup>65</sup> plant phospholipase,<sup>57</sup> and  $Na^+/K^+$ -ATPase,<sup>69</sup> whose activities are highly dependent on the binding of  $Ca^{2+}$  with anionic lipids. However, detailed regulation mechanisms of  $Ca^{2+}$  ions need to be further validated by experiments.

## Conclusions

The present MD simulations have provided a new insight into the effects of  $Na^+$ ,  $K^+$ , and  $Ca^{2+}$  ions and their mixture on the structural properties of anionic lipid bilayer in general, and the POPG bilayer in particular. The MD simulations fully addressed the interactions of these ions with the POPG bilayer. In particular, our MD simulations allow for the following conclusions. First, long-time effects of these ions on the structure of POPG bilayer have been addressed. Different from the conclusion driven from the short time MD simulations,<sup>32</sup> our submicrosecond MD simulations revealed that there is no pronounced difference between the effects of  $Na^+$  and  $Ca^{2+}$  ions on the structure of POPG bilayer when the ions are treated as counterions. Second, the three ions display different behaviors in regulating the structure of POPG bilayer. As counterions,  $K^+$  ions only show weak effects on the structure of POPG bilayer, while both  $Na^+$  and  $Ca^{2+}$  ions could tighten the structure of POPG bilayer, making the lipid headgroups to be more vertical with respective to the membrane surface and increasing the ordering of the lipid tails. Third, either the extra  $Ca^{2+}$  ions or  $Ca^{2+}$  ions in the ion mixture show special effects on the structure of POPG bilayer. The extra  $Ca^{2+}$  ions perform further influence on the POPG bilayer by stabilizing and tightening the membrane structure, whereas the extra  $Na^+$  ions do not.  $Ca^{2+}$  ions in the ion mixture display dominative effects on the structure of POPG bilayer and the binding of  $Na^+$  and  $K^+$  ions to lipids is greatly inhibited by  $Ca^{2+}$  ions. Consequently, some biological implications of  $Ca^{2+}$  effects on the structures of anionic lipid bilayers are proposed whereby our MD simulation results can be used to explain the action mechanisms of several membrane proteins, receptors, and ion channels. In future studies, more attention should be paid to larger systems and more complicated ion compositions.

**Acknowledgment.** This work is supported by the National Natural Science Foundation of China (20720102040 and 20721003), State Key Program of Basic Research of China (2009CB918502), National S&T Major Project (2009ZX09501-001), China Postdoctoral Science Foundation grants (200902262), and Information Construction Project of Chinese Academy of Sciences (No.INFO-115-B01). Computational resources were supported by the Computer Network Information Center (CNIC) of the Chinese Academy of Sciences (CAS) and by the Shanghai Supercomputing Center (SCC).

## References and Notes

- (1) Castleden, J. A. *J. Pharm. Sci.* **1969**, *58*, 149.
- (2) Bangham, A. D. *Prog. Biophys. Mol. Biol.* **1968**, *18*, 29.
- (3) Spector, A. A.; Yorek, M. A. *J. Lipid Res.* **1985**, *26*, 1015.
- (4) Farias, R. N.; Bloj, B.; Morero, R. D.; Sineriz, F.; Trucco, R. E. *Biochim. Biophys. Acta* **1975**, *415*, 231.
- (5) Qin, Z.; Tepper, H. L.; Voth, G. A. *J. Phys. Chem. B* **2007**, *111*, 9931.
- (6) Tari, A.; Huang, L. *Biochemistry* **1989**, *28*, 7708.
- (7) Brotherus, J. R.; Jost, P. C.; Griffith, O. H.; Keana, J. F.; Hokin, L. E. *Proc. Natl. Acad. Sci. U. S. A.* **1980**, *77*, 272.
- (8) Brasseur, R.; Laurent, G.; Ruysschaert, J. M.; Tulkens, P. *Biochem. Pharmacol.* **1984**, *33*, 629.
- (9) Petrou, S.; Ordway, R. W.; Hamilton, J. A.; Walsh, J. V., Jr.; Singer, J. J. *J. Gen. Physiol.* **1994**, *103*, 471.
- (10) Parsegian, V. A. *Ann. N. Y. Acad. Sci.* **1975**, *264*, 161.
- (11) Watts, A.; Harlos, K.; Marsh, D. *Biochim. Biophys. Acta* **1981**, *645*, 91.
- (12) Hauser, H.; Shipley, G. G. *Biochemistry* **1984**, *23*, 34.
- (13) Loosley-Millman, M. E.; Rand, R. P.; Parsegian, V. A. *Biophys. J.* **1982**, *40*, 221.
- (14) Akutsu, H.; Seelig, J. *Biochemistry* **1981**, *20*, 7366.
- (15) Clarke, R. J.; Lup fert, C. *Biophys. J.* **1999**, *76*, 2614.
- (16) Bockmann, R. A.; Hac, A.; Heimborg, T.; Grubmuller, H. *Biophys. J.* **2003**, *85*, 1647.
- (17) Sachs, J. N.; Crozier, P. S.; Woolf, T. B. *J. Chem. Phys.* **2004**, *121*, 10847.
- (18) Bockmann, R. A.; Grubmuller, H. *Angew. Chem., Int. Ed. Engl.* **2004**, *43*, 1021.
- (19) Gurtovenko, A. A.; Miettinen, M.; Karttunen, M.; Vattulainen, I. *J. Phys. Chem. B* **2005**, *109*, 21126.
- (20) Gurtovenko, A. A.; Vattulainen, I. *Biophys. J.* **2007**, *92*, 1878.
- (21) Lee, S. J.; Song, Y.; Baker, N. A. *Biophys. J.* **2008**, *94*, 3565.
- (22) Cordomi, A.; Edholm, O.; Perez, J. J. *J. Phys. Chem. B* **2008**, *112*, 1397.
- (23) Herrera, F. E.; Pantano, S. *J. Chem. Phys.* **2009**, *130*, 195105.
- (24) Shinoda, K.; Shinoda, W.; Mikami, M. *Phys. Chem. Chem. Phys.* **2007**, *9*, 643.
- (25) Pabst, G.; Hodzic, A.; Strancar, J.; Danner, S.; Rappolt, M.; Laggner, P. *Biophys. J.* **2007**, *93*, 2688.
- (26) Binder, H.; Zschornig, O. *Chem. Phys. Lipids* **2002**, *115*, 39.
- (27) Garcia-Manyes, S.; Oncins, G.; Sanz, F. *Biophys. J.* **2005**, *89*, 1812.
- (28) Petrache, H. I.; Tristram-Nagle, S.; Harries, D.; Kucera, N.; Nagle, J. F.; Parsegian, V. A. *J. Lipid Res.* **2006**, *47*, 302.
- (29) Pandit, S. A.; Berkowitz, M. L. *Biophys. J.* **2002**, *82*, 1818.
- (30) Mukhopadhyay, P.; Monticelli, L.; Tielemans, D. P. *Biophys. J.* **2004**, *86*, 1601.
- (31) Bhide, S. Y.; Zhang, Z.; Berkowitz, M. L. *Biophys. J.* **2007**, *92*, 1284.
- (32) Pedersen, U. R.; Leidy, C.; Westh, P.; Peters, G. H. *Biochim. Biophys. Acta* **2006**, *1758*, 573.
- (33) Elmore, D. E. *FEBS Lett.* **2006**, *580*, 144.
- (34) Zhao, W.; Rog, T.; Gurtovenko, A. A.; Vattulainen, I.; Karttunen, M. *Biophys. J.* **2007**, *92*, 1114.
- (35) Pimthon, J.; Willumeit, R.; Lendlein, A.; Hofmann, D. *J. Mol. Struct.* **2009**, *921*, 38.
- (36) Humphrey, W.; Dalke, A.; Schulten, K. *J. Mol. Graph.* **1996**, *14*, 33.
- (37) Berendsen, H. J. C.; Grigera, J. R.; Straatsma, T. P. *J. Phys. Chem.* **1987**, *91*, 6269.
- (38) Hess, B.; Kutzner, C.; Spoel, D.; Lindahl, E. *J. Chem. Theory Comput.* **2008**, *4*, 435.
- (39) Chakrabarti, N.; Neale, C.; Payandeh, J.; Pai, E. F.; Pomes, R. *Biophys. J.* **2010**, *98*, 784.
- (40) Berger, O.; Edholm, O.; Jahnig, F. *Biophys. J.* **1997**, *72*, 2002.
- (41) Egberts, E.; Marrink, S. J.; Berendsen, H. J. *Eur. Biophys. J.* **1994**, *22*, 423.
- (42) Chiu, S. W.; Clark, M.; Balaji, V.; Subramaniam, S.; Scott, H. L.; Jakobsson, E. *Biophys. J.* **1995**, *69*, 1230.
- (43) Lindahl, E.; Edholm, O. *Biophys. J.* **2000**, *79*, 426.
- (44) Kaminski, G. A.; Friesner, R. A. *J. Phys. Chem. B* **2001**, *105*, 6474.
- (45) Miyamoto, S.; Kollman, P. A. *J. Comput. Chem.* **1992**, *13*, 952.
- (46) Hess, B.; Bekker, H.; Berendsen, H. J. C.; Fraaije, J. G. E. M. *J. Comput. Chem.* **1998**, *18*, 1463.
- (47) Essmann, U.; Perera, L.; Berkowitz, M. L.; Darden, T.; Lee, H.; Pedersen, L. G. *J. Chem. Phys.* **1995**, *103*, 8577.
- (48) Berendsen, H. J. C.; Postma, J. P. M.; van Gunsteren, W. F.; DiNola, A.; Haak, J. R. *J. Chem. Phys.* **1984**, *81*, 3684.
- (49) Bussi, G.; Donadio, D.; Parrinello, M. *J. Chem. Phys.* **2007**, *126*, 014101.
- (50) Dickey, A.; Faller, R. *Biophys. J.* **2008**, *95*, 2636.
- (51) Tielemans, D. P.; Marrink, S. J.; Berendsen, H. J. *Biochim. Biophys. Acta* **1997**, *1331*, 235.
- (52) Song, Y.; Guallar, V.; Baker, N. A. *Biochemistry* **2005**, *44*, 13425.
- (53) Gregory, D. P.; Mingins, J.; Smith, A. L. *Colloids Surf. B* **1985**, *14*, 303.
- (54) Hauser, H.; Dawson, R. M. *Eur. J. Biochem.* **1967**, *1*, 61.
- (55) Bockmann, R. A.; Hac, A.; Heimborg, T.; Grubmuller, H. *Biophys. J.* **2003**, *85*, 1647.
- (56) Silvius, J. R. *Biochemistry* **1990**, *29*, 2930.
- (57) Kuppe, K.; Kerth, A.; Blume, A.; Ulrich-Hofmann, R. *Chembiochem* **2008**, *9*, 2853.
- (58) Leventis, R.; Gagne, J.; Fuller, N.; Rand, R. P.; Silvius, J. R. *Biochemistry* **1986**, *25*, 6978.
- (59) Binder, W. H.; Barragan, V.; Menger, F. M. *Angew. Chem., Int. Ed. Engl.* **2003**, *42*, 5802.
- (60) Ross, M.; Steinem, C.; Gallia, H.; Janshoff, A. *Langmuir* **2001**, *17*, 2437.

- (61) Orrenius, S.; Zhivotovsky, B.; Nicotera, P. *Nat. Rev. Mol. Cell Biol.* **2003**, *4*, 552.
- (62) Tait, J. F.; Gibson, D. *Arch. Biochem. Biophys.* **1992**, *298*, 187.
- (63) Verdaguer, N.; Corbalan-Garcia, S.; Ochoa, W. F.; Fita, I.; Gomez-Fernandez, J. C. *EMBO J.* **1999**, *18*, 6329.
- (64) Janshoff, A.; Ross, M.; Gerke, V.; Steinem, C. *Chembiochem* **2001**, *2*, 587.
- (65) Walther, M.; Wiesner, R.; Kuhn, H. *J. Biol. Chem.* **2004**, *279*, 3717.
- (66) Zurborg, S.; Yurgionas, B.; Jira, J. A.; Caspani, O.; Heppenstall, P. A. *Nat. Neurosci.* **2007**, *10*, 277.
- (67) Doerner, J. F.; Gisselmann, G.; Hatt, H.; Wetzel, C. H. *J. Biol. Chem.* **2007**, *282*, 13180.
- (68) Sokabe, T.; Tsujuchi, S.; Kadokawa, T.; Tominaga, M. *J. Neurosci.* **2008**, *28*, 9929.
- (69) Dalskov, S. M.; Immerdal, L.; Niels-Christiansen, L. L.; Hansen, G. H.; Schousboe, A.; Danielsen, E. M. *Neurochem. Int.* **2005**, *46*, 489.

JP1091569